THE INFLUENCE OF TURBULENCE INTENSITY ON THE FLOW STRUCTURE OVER A THIN AIRFOIL AT LOW REYNOLDS NUMBERS

Sridhar Ravi#, Simon Watkins*, Jon Watmuff*, Phred Petersen* and Matthew Marino*
#University of Tuebingen, *RMIT University
sridhar.ravi@uni-tuebingen.de, simon@rmit.edu.au

Abstract

Large-scale freestream turbulence commonly present within the atmosphere poses significant challenges to the flight of Micro Air Vehicles. In order to examine the influence of turbulence intensity on the loads occurring over an airfoil, two turbulence conditions of nominally the same longitudinal integral length scale (Lxx/c = 1) but with significantly different intensities (Ti = 7.2% & 12.3%) were generated within a wind tunnel and time-varying surface pressure measurements and smoke flow visualization were made on a thin flat-plate airfoil at Reynolds number relevant to MAV flight. At lower angles of attack, the rapid changes in oncoming flow velocity and direction rendered a large variation in instantaneous flow structure over the airfoil, consequently leading to a significant increase in surface pressure fluctuations. At higher angles of attack, flow-field over the airfoil was noted to be considerably different whereby enhanced roll-up of the leading edge separated shear layer occurred. This resulted in the formation of large Leading Edge Vortices which had a significant influence on the aerodynamic loads experienced by the airfoil. The rate of LEV formation was dependent on the angle of attack until 10° and it was independent of the turbulence properties tested.

1 Introduction

Micro air vehicles (MAVs) are currently of interest for use in military and civilian operations due to their potential for surveillance and information gathering [1]. Their general role will be to operate where direct line of sight is not available (from either a person or a larger manned, or unmanned, craft) and they will operate at low altitude and usually in complex terrain. MAVs will thus be flown very slowly (Figure 1) in the lower levels of the turbulent atmospheric boundary layer (ABL). This region of the atmosphere is highly turbulent on days when there is any appreciable atmospheric wind and this turbulence presents a significant challenge to any craft, artificial or natural,. Developing a MAV that can maintain a stable in complex terrain within the ABL is a challenge, and one that must be overcome if MAVs are to be successfully utilized in the field if their operation is not limited to "fair weather use only". Consequently the environment is emerging as a major constraint on the operations of MAVs with an increasing vulnerability to turbulence as size and speed reduces [2]. Due to their small size, low flight speed and operating conditions, MAVs in flight would be exposed to both low Reynolds number effects as well as of large-scale freestream turbulence.

Considerable research has been conducted in order to understand airfoil performance in smooth flow at Re > 500,000. However, recent demands for superior and more versatile MAVs has urged researcher to study the flow structure over airfoils at much lower Re (50,000 < Re < 200,000) as well. Under smooth flow conditions, airfoil performance has been found to deteriorate considerably in this flow regime [3 & 4]. This reduction in aerodynamic performance has been attributed to the extended laminar region that is usually present over airfoils at these Reynolds numbers. In the presence of an Adverse Pressure Gradient (APG) premature separation of the laminar

shear layer has also been observed to occur whereby, the separated shear layer transitions and reattaches further downstream as a turbulent boundary layer. The region between the laminar separation and turbulent reattachment is commonly referred to as a Laminar Separation Bubble (LSB). The presence and structure of a LSB and other associated flow phenomena have a significant influence on overall aerodynamic performance [4 - 7].

A wide range of turbulent flow conditions is experienced outdoors, due to the wide range of atmospheric wind-speeds, flight speeds and terrain conditions. The influence of turbulence on the aerodynamic characteristic of MAV wings and airfoils is still unclear. Only limited literature exists on the flow structure over airfoils subjected to such elevated levels of freestream turbulence at Reynolds numbers relevant to MAVs. A number of other researchers [8 – 12] have assessed airfoil performance in high levels of freestream turbulence; however their results are more relevant to turbine blades as the experiments were conducted at Reynolds numbers significantly higher than the MAV operational range. Wind engineers have conducted a number of studies on the influence of turbulence on the flow structure over bluff bodies (e.g flat-plates, cuboids etc.) for many decades and have noted the influence of turbulence intensity and integral length scale; however whilst some testing was conducted at Reynolds numbers relevant to MAVs, the results are more suited to the aerodynamics of tall building and bridges [13 – 16]. Mueller [17] investigated the influence of elevated levels of turbulence on airfoils, but these were at significantly lower turbulence levels than generally present within the ABL and at very low integral length scales.

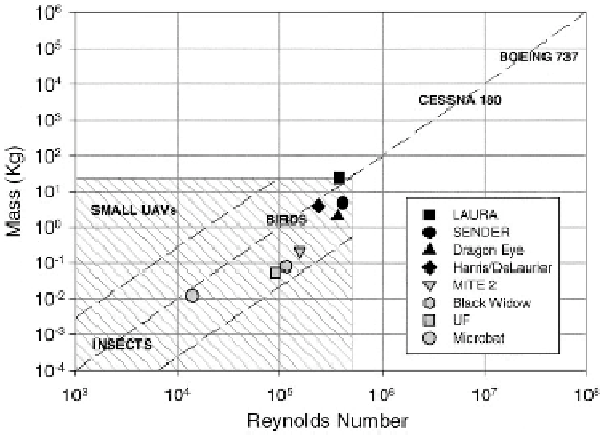

Figure 1 - Relative Reynolds number environment of small UAVs and MAVs. (source: Mueller [4])

The work presented in this paper provides insights on the influence of turbulence intensity on the forces and flow structure occurring over the airfoil at Reynolds numbers relevant to MAV flight through the ABL. Surface pressure measurements at multiple chordwise stations and smoke flow visualizations were conducted to study the transient flow structure over the airfoil.

2 Experiment Setup and Instrumentation

A thin flat plate airfoil with an elliptical leading edge and tapered trailing edge was chosen for the experiments described here. The airfoil was 1.9% thick and its chord was set to 150 mm. A side view of airfoil section is presented in Figure 2. This airfoil section was chosen because its mean and transient performance in nominally smooth has been well documented through surface pressure and force measurements made by Ravi [18&19] and Mueller [4] respectively. The span was set to 900 mm, such that the end-plates would not influence the oncoming turbulent eddies. This resulted in an AR = 6, which is around the same AR used by Swalwell [12]. Circular end plates enabled pitching about center chord which in turn fitted into the walls of an airfoil mount. The airfoil mount consisted of an open-roofed “box” with relatively thin horizontal slats placed on top to improve structural rigidity when exposed

to turbulent flows, see Figure 3. One side of the airfoil mount the circular end-plate was made of transparent Perspex to serve as a chordwise viewing window.

To keep the airfoil out of ground-effect, the airfoil was located four chord lengths above the base of the mount. Side walls of the mount extended to three chord lengths above the airfoil location and four chord lengths to the rear of the airfoil to achieve a nominally two dimensional flow (Figure 3). In order to reduce the influence of the airfoil mount walls on the oncoming turbulent eddies, the airfoil was placed such that the Leading Edge (LE) was half chord length from the front edge of the mount. In this setup, it was considered that the turbulent eddies should impinge the airfoil well before being significantly influenced by the boundaries of the supporting structure. To stay away from the boundaries of the wind tunnel the airfoil mount was placed in the center of the test section over a platform raised by four chord lengths.

The airfoil was manufactured using a rapid prototyping method with integral surface pressure taps. Pressure measurements were made using the Dynamic Pressure Measurement System (DPMS) manufactured by Turbulent Flow Instrumentation (TFI) [20]. This system digitally measures pressure signals on 60 channels. Due to practical considerations the tapped airfoil consisted of 40 channels. Tubing of 1mm ID was then used to connect the integral pressure taps to DPMS module. The total tubing length from pressure tap to transducer was 600 mm. Dynamic corrections, based on the work of Bergh and Tijdeman [21], was applied to the tubing system to enhance the frequency response giving an essentially flat amplitude response to a few hundred hertz. Since the frequencies of interest here at typically under 100Hz, this response was deemed sufficient. Digital data acquisition was by a National Instruments 6032E DAQ card in a PC.

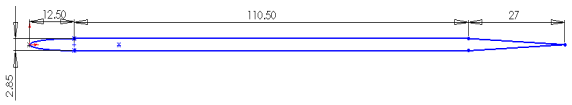

Figure 2: Side view of airfoil section with dimensions in mm, [18]

2.1 *RMIT University Industrial Wind Tunnel*

Testing was performed in the RMIT 2x3x9m closed jet, closed test section Industrial Wind Tunnel (IWT) which was configured to generate turbulence using a series of grids. In its clean configuration (without grids), the wind-tunnel had a base turbulence intensity of around 1.2%. Discussion of the loads over the airfoil under smooth flow conditions will not be presented here as it has been presented in significant detail in Ravi [18&19]. Planar grid of panel width 300 mm at 600 mm inter-panel spacing were placed at the inlet of the contraction section of the wind tunnel to produce turbulence of intensity of around 12.3% and length scales measuring 0.15m, 0.10m and 0.09m in the longitudinal, lateral and vertical directions respectively. In order to identify the influence of Ti, another grid of 30 mm panel width and 30 mm inter-panel spacing was placed at the inlet of the test section to produce turbulence of intensity of around 7.2% and length scales measuring 0.15m, 0.06m and 0.08m in the longitudinal, lateral and vertical directions respectively at 5.5 m downstream from the grids. The integral length scales were estimated using both von Karman spectral fitting and the autocorrelation methods, very good agreement between them was observed, Ravi [22]. While there may exist an infinite combination of turbulence intensity and length scales, these particular turbulence conditions were chosen since the longitudinal integral length scales were nominally the same (i.e. comparable to the airfoil chord) and the turbulence intensities were considerably different.

Figure 3 – Pressure tapped airfoil between end plates and upstream of grids in RMIT IWT

For the flow visualization experiments, the smoke generator at RMIT was used. The generator produced white smoke by pumping mineral oil through a hot wand. A different airfoil made from Aluminum with similar geometric properties as that used for pressure measurements was used for the flow visualization tests. The Phantom V4.3 high speed camera manufactured by Vision Research was used to capture the path of the smoke infused within the flow. In the tests, the wand was placed 0.5c upsteam of the leading edge. Sensitivity studies showed that the wand did not have any notable influence on the pressure fluctuations over the airfoil, due to the rapid breakdown of disturbances induced by the wand. Smoke visualization was conducted from top, side and rear vantage points to reveal not only chordwise, but also the spanwise structure of the flow.

3 Results

3.1 Mean and Standard Deviation of Surface Pressures

The surface pressures and flow over the airfoil when Ti = 7.2% Lxx = 0.14m and Ti = 12.3% Lxx = 0.15m were compared to examine the influence of changes in Ti on aerodynamic loads occurring over the airfoil. As the longitudinal integral length scales in both turbulence conditions were nominally the same, and all other parameters were unchanged, any differences in the pressure distribution may be attributed to the influence of change in Ti.

At lower AoAs (AoA = 0°- 4°), the influence of Ti on the mean C_P distribution is hardly noticeable as seen in Figure 4&5. At 4° AoA, compared to when Ti = 12.3% higher suction is created close to the LE when Ti = 7.2% while pressure distribution over majority of the airfoil remained similar. In both cases, the peak suction is significantly lower than that observed in nominally smooth flow where the minimum mean C_P, close to the LE, at the same AoA was around -1.4 [18&19]. The σ_{Cp} distribution (Figure 7&8) shows considerable differences in the magnitude of fluctuations occurring over the airfoil in the two turbulence conditions. Between 0°- 4° AoAs, σ_{Cp} is much higher close to the LE when Ti = 12.3% as opposed to the Ti = 7.2% condition. Increase in Ti meant an increase in the magnitude of ambient disturbances and changes in the instantaneous AoA, consequently the airfoil experienced higher pressure fluctuation when Ti = 12.3%.

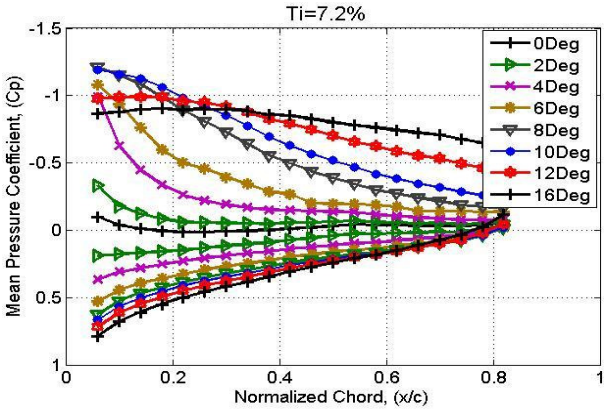

Figure 4: Mean C_P distribution over the airfoil top and bottom surface between 0-16° AoA. When Ti=7.2%

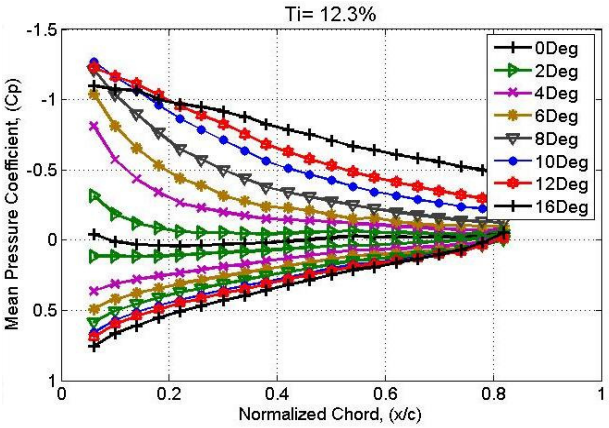

Figure 5: Mean C_P distribution over the airfoil top and bottom surface between 0-16° AoA. When Ti=12.3%

It was identified through the smoke flow visualization that the flow over the airfoil was very dynamic under elevated turbulence. For both turbulence conditions, at lower AoAs (<4°) the shear layer over the airfoil alternated between a separated and attached profile (Figure 6). Flow separation generally occurred at the LE and it was always accompanied by downstream reattachment. At such instances an "instantaneous" separation bubble formed. The

separation bubbles occasionally formed over the airfoil, but they stayed over the chord only for very short durations before the flow reverted to fully attached condition. These instantaneous separation bubbles at lower AoAs have been attributed to the local pitch angle fluctuations experienced by the airfoil under high turbulence levels.

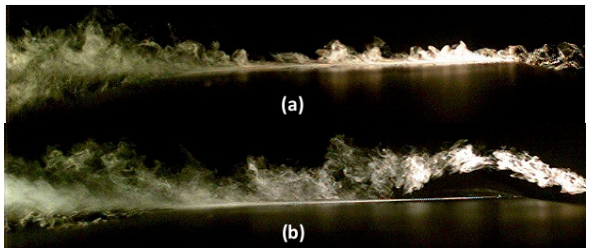

Figure 6: Figures a & b shows variation in flow structure over the airfoil at 2° AOA when Ti=12.3%. [18]

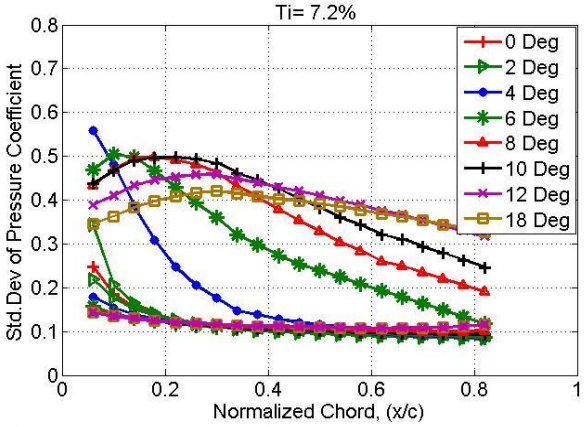

Figure 7: Standard deviation of C_P distribution over the airfoil top and bottom surface between 0-16° AoA. When Ti=7.2%

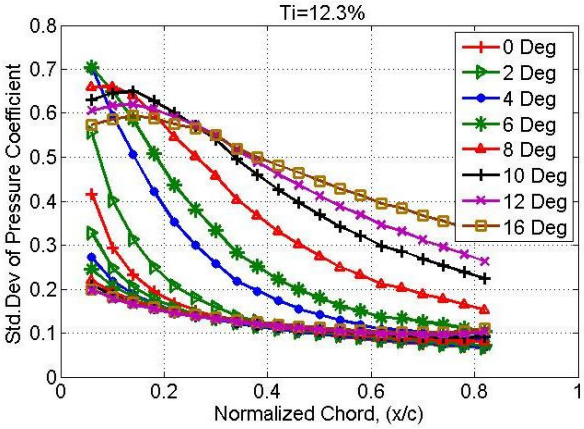

Figure 8: Standard deviation of C_P distribution over the airfoil top and bottom surface between 0-16° AoA. When Ti=12.3%

For AoAs above 4°, a laminar separation bubble formed over the airfoil in smooth flow conditions, which imparted a region of constant mean C_P near the LE [18&19]. Under elevated turbulence levels, this region was missing and rapid pressure recovery ensued even at higher AOAs (Figure 4&8). At AoA > 8° when Ti=7.2%, a small region of constant mean C_P is noticed close to the LE while a rapid pressure recovery occurs at even 10° AoA when Ti=12.3%, see Figure 4&5. For AoAs > 6° the σ_{Cp} distribution when Ti = 7.2% (Figure 7) has some similarity with that observed in nominally smooth flow whereby the σ_{Cp} is seen to increase over the chord until it reaches maximum then stabilizes before decreasing.

At AoAs > 6°, the flow visualizations revealed that in high levels of freestream turbulence, when the LE encountered an increase in pitch angle, flow separation occurred from the LE similar to smooth flow conditions. But unlike in smooth flow, enhanced roll up of the shear layer was observed (Figure 9). This may be attributed to the increased levels of ambient unsteadiness when Ti was high. The enhanced shear layer roll-up could be seen to induce the formation of strong Leading Edge Vortices (LEVs), akin to those occurring over a dynamically stalling airfoil. As there is still much uncertainty about the vortices observed here, direct comparisons with the LEVs observed over dynamically stalling airfoils will not be made. However, the LEVs seen here greatly differed from LSBs (observed to form over the airfoil in smooth flow conditions [18&19] since significantly higher flow circulation and pulsating cycles of rapid growth and dispersion were present in the former. In nominally smooth flow condition, LEVs never formed as only relatively limited sections of the shear layer rolled up as recirculating fluid, while some of the fluid proceeded over the bubble. Inside the LSB, fluid entrainment and circulation has been reported to be relatively mild.

Figure 9: Leading edge separation and enhanced shear layer roll up, leading to the formation of a vortex. AoA = 10Deg, Ti=12.3. [18]

At higher AoAs (AoA > 10°) the peak suction can be noted to rise with increase in Ti (Figure 7&8). As Ti increased it was considered that the airfoil experienced longer periods of attached flow condition through the formation of the LEVs. Though the formation of LEVs generally implies that flow detachment has already transpired, rapid pressure recovery is still experienced by the shear layer which is akin to that observed when the shear layer remains attached. The greater resistance offered to the APG by the significantly more energetic shear layer and closer proximity of the same to the airfoil surface in elevated levels of turbulence (due to the increased rollup) rendered a greater suction than that experienced when the shear layer remained fully detached (i.e. stalled condition). For Ti = 7.2%, the airfoil stalled at around 14° where the mean C_P was relatively constant over the entire chord. This is considerably higher than the stall angle in nominally smooth flow (10°), Ravi [18&19]. The σ_{Cp} distribution (Figure 7&8) however indicated that the location of maximum fluctuation moved downstream only to a limited extent with increase in AoA. Unlike in smooth flow, where at the stalling AoA the location of $\sigma_{Cp(max)}$ was near the TE (Ravi [18&19]), when Ti=7.2% at AoA=14° $\sigma_{Cp(max)}$ was at around 0.3 *(x/c)* (Figure 7). In elevated levels of Ti, the location of $\sigma_{Cp(max)}$ appeared to correlate well with the region shear layer reattachment during the formation of LEVs. The peak in σ_{Cp} became less acute with increase in AoA implying that the location where the LEVs formed oscillated over a greater region at higher AoAs. In comparison, when Ti = 12.3% (Figure 5&8), a decrease in minimum mean C_P is noticed as AoA increases, however the region of peak suction remains near the LE throughout the range of AoA presented. Even when AoA = 18° no sign of stall was present with the location of $\sigma_{Cp(max)}$ remaining close to LE. The increased Ti seemed to amplify the LEVs, further delaying stall and increasing the fluctuations experienced.

In both smooth and turbulent flow, the mean C_P and σ_{Cp} converged to a similar distribution on the pressure side (Figures 4, 5, 7&8). While the mean C_P distribution was also very similar in all flow conditions (i.e. smooth and turbulent), the σ_{Cp} increased to around 0.15 C_P when Ti=12.3% from 0.02 C_P in Ti=1.2% condition. The lack of change in C_P distribution on the airfoil pressure side implies that as AoA increases and the underside "faces" the oncoming flow, due to the favorable pressure gradient the fluctuations in oncoming pitch angle have a significantly reduced influence.

3.2 Spectral Analysis of Surface Pressures

At lower geometric angles of attack (AoA > 4°), the surface pressure fluctuations were generally random in both turbulence conditions. Considering that the oncoming fluctuations in pitch angle and velocity are completely stochastic it is likely that the pressure fluctuations would also be random.

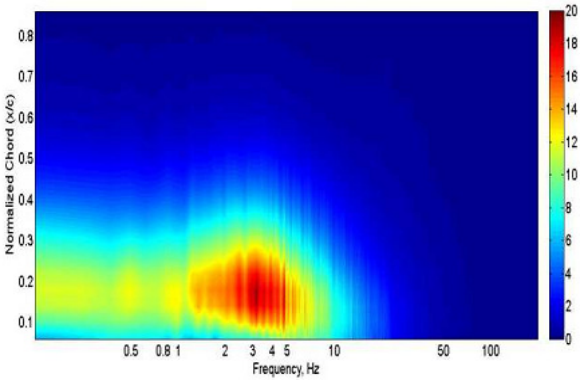

Figure 10: Consolidated spectra of pressure fluctuations occurring over airfoil at AoA 6°. Ti=7.2%, Lxx/c=1. Re=75000

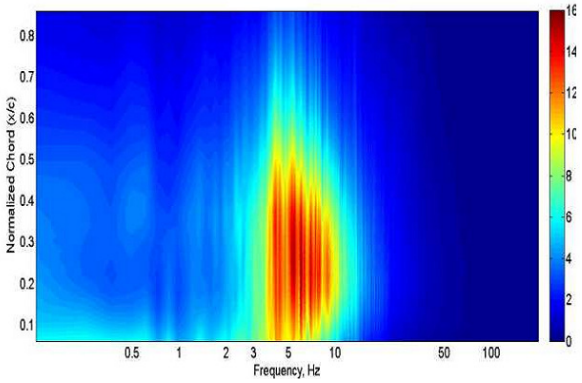

Figure 11: Consolidated spectra of pressure fluctuations occurring over airfoil at AoA 10°. Ti=7.2%, Lxx/c=1. Re=75000

As α was increased to 6°, relatively higher pressure fluctuations occurred between *(x/c)* = 0.1 - 0.25 along with an increase in energy (not present at lower angles of attack) at $f \approx 3.5$Hz (Figure 10). With further increase in α, the chordwise region experiencing maximum pressure fluctuation moved towards the TE and the frequency range at which maximum oscillations occurred also increased, Figure 11.

For Ti=12.3%, similar to the lower turbulence intensity condition, as α was increased above 6° the frequency range at which maximum fluctuations occurred became narrower compared to the spectra of pressures when α < 6° where a broadband increase in fluctuations at lower wave numbers was present, Figure 12&13. The wave number range of peak fluctuations for angles of attack > 6° was also very similar to that present when Ti was 7.2%. However, the chordwise location experiencing maximum fluctuations remained consistently closer to the LE. It is therefore believed that for α > 6°, a similar flow structure may be present over the airfoil in both turbulence conditions, however when Ti = 12.3%, an earlier onset (along the chord) of the observed fluctuations occurred.

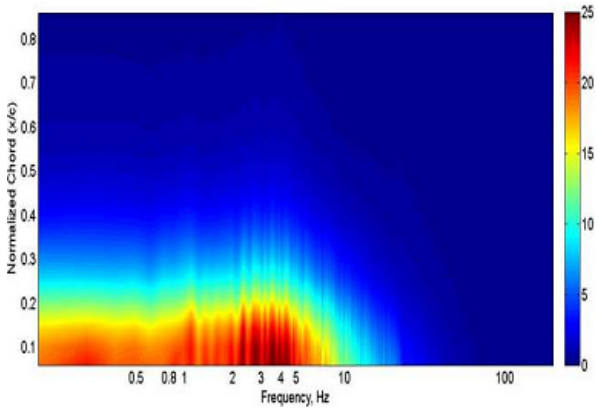

Figure 12: Consolidated spectra of pressure fluctuations occurring over airfoil at AoA 6°. Ti=12.3%, Lxx/c=1. Re=75000

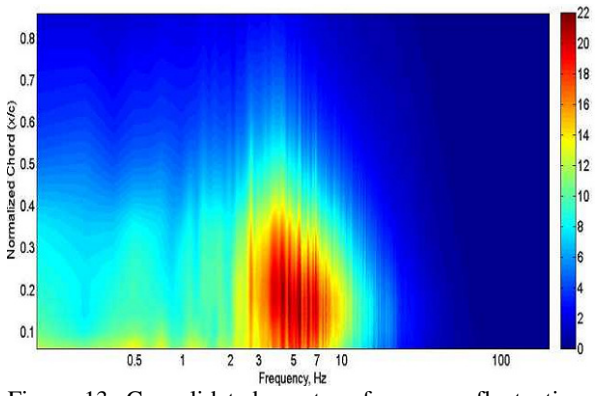

Figure 13: Consolidated spectra of pressure fluctuations occurring over airfoil at AoA 10°. Ti=12.3%, Lxx/c=1. Re=75000

The comparison between the peak in the spectra of surface pressures and the respective time series identified that the increase in energy in the pressure spectra at α > 6° (refer Figure 11-13) corresponded to the average rate of LEV formation and shedding. The spectra of pressures measured at location of maximum oscillation for various AOAs are plotted in Figure 14&15. It clearly shows that the frequency peak increases with AOA till around 10° after which it remains nominally constant. The shedding frequency wave number $(\mu = f \times c/v)$ versus AOA for both turbulence intensities is plotted in Figure 16. Due to the diminished spectral resolution, a line of best fit was passed through the spectra to effectively determine the most appropriate spectral peak for each AOA in Figure 16. The Increase in LEV formation rate with increase in AoA is believed to be due to the higher instantaneous angles of

attack and the increased instability of the shear layer in the presence of a stronger adverse pressure gradient. Further measurements on the shear layer structure are required to ascertain this. The change in LEV formation rate with change in AoA is also believed to be a property of the airfoil geometry and the integral length scale, the fact that a similar trend is noticed at higher turbulence intensity further supports this.

The airfoil stalls much later in turbulence whereby due to the fluctuations, instances of attached flow condition was noticed even when AOA=16Deg. No distinct peak was visible in the pressure spectra even at 20Deg AOA. Flow visualization however showed that bluff body like vortex shedding occurs only intermittently i.e. when the instantaneous AOA is high enough to enable the same.

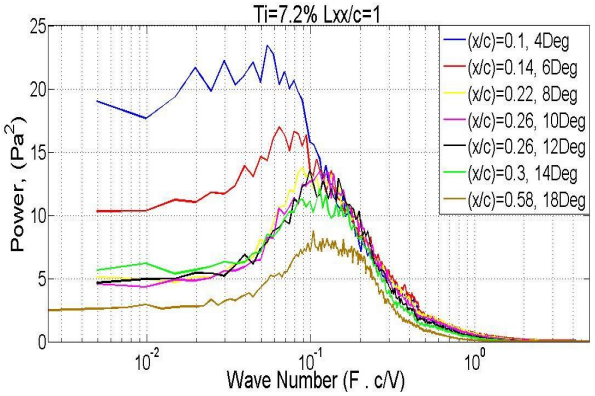

Figure 14 – Spectra of pressures measured at location of maximum oscillation at various AOAs when Ti=7.2%. [23]

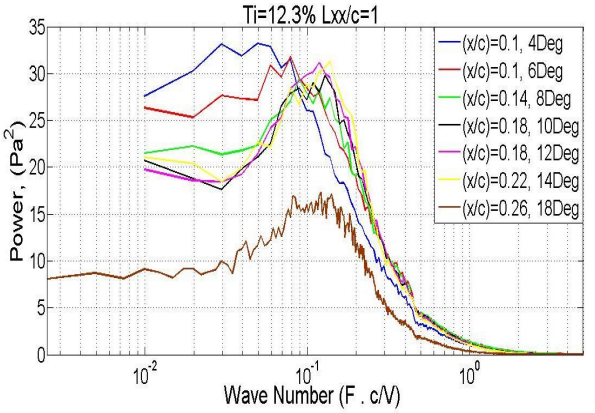

Figure 15 – Spectra of pressures measured at location of maximum oscillation at various AOAs when Ti=12.3%. [23]

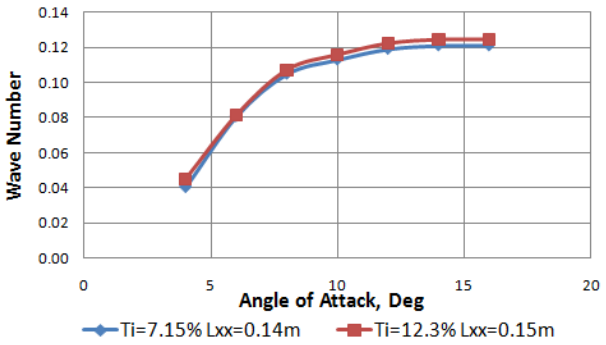

Figure 16: Wave number ($\mu = f \times c/u$) at which LEVs formed at different α using chord as representative length. [23]

4 Conclusions

The influence of turbulence intensity on the flow structure over a thin airfoil was investigated by taking time-varying surface pressures at multiple chordwise stations. The longitudinal integral length scales in the two turbulence conditions were nominally the same (Lxx/c = 1) while the turbulence intensities was significantly different (Ti = 7.2% & 12.3%). At lower AoAs the flow structure was very dynamic and this imparted large pressure fluctuations over the airfoil. Highest suction was present close to the leading and rapid pressure recovery ensued, this trend was noted to occur even at higher AoAs. At geometric angles of attack > 6° strong LEVs were formed due to the enhanced roll-up of the leading-edge separated shear layer. The shear layer reattachment region (i.e. origin of the LEV) correlated well with the region experiencing maximum pressure fluctuations. For both turbulence conditions, the rate of formation of LEVs was dependent on the geometric α until 10° after which the formation rate remained nominally constant at a $\mu \approx 0.12$. The images from flow visualizations and surface pressures provided strong indication that the LEV formation rates maybe a characteristic of the airfoil section and dependent on the angle of attack and the integral length scale.

5 Acknowledgments

The authors thank AFOSR, RMIT MAV research group and RMIT technical support staff for their assistance.

6 References

[1] Anon, 'UAVs Applications are Driving Technology – Micro Air Vehicles', UAV Annual Report, Defense Airborne Reconnaissance Office, Pentagon, Washington, 6 November (1997), p.32.

[2] Spedding, G.R., and Lissaman, P.B.S., "Technical Aspects of Microscale Flight Systems", Journal of Avian Biology, (1998) Vol. 29, No. 4, pp.458-468.

[3] Carmichael, B.H., "Low Reynolds Number Airfoil Survey." Volume I, NASA Contractor Report 165803, 1981.

[4] Mueller, T.J., "Aerodynamic Measurements at Low Reynolds Numbers for Fixed Wing Micro-Air Vehicles." Proceedings of the Development and Operation of UAVs for Military and Civil Applications Short Course. Belgium: published in Rto-EN-9 by NATO, April 2000, 1999.

[5] Watmuff, J. H., "Evolution of a wave packet into vortex loops in a laminar separation bubble." J. Fluid Mech. (1999) Vol. 397: 119–169.

[6] Gaster. M., "The structure and behaviour of laminar separation bubbles". AGARD CP-4, 1966, 813–854.

[7] Roberts, W.B., "Calculation of laminar separation bubbles and their effect on airfoil performance." AIAA Journal. Vol. 18, no. 1 (1980): 25-31.

[8] Stack, J., "Tests in the Variable Density Wind Tunnel to Investigate the Effects of Scale and Turbulence on Airfoil Characteristics". NACA-TN-364(1931), NACA Langley Memorial Aeronautical Laboratory

[9] Jancauskas, E. D., "The Cross-Wind Excitation of Bluff Structures and the Incident Turbulence Mechanism." Doctoral thesis, Monash University, Clayton, (1983)

[10] Devinant, P., Laverne, T. and Hureau, J., "Experimental study of wind-turbine airfoil aerodynamics in high turbulence." Journal of Wind Engineering and Industrial Aerodynamics. (2002) Vol. 90: 689-707

[11] Sicot, C., Aubrun, S., Loyer, S.and Devinant, P., "Unsteady characteristics of the static stall of an airfoil subjected to freestream turbulence level up to 16%." Experiments in Fluids. (2006) Vol. 41: 641-648.

[12] Swalwell, K., "The Effect of Turbulence on Stall of Horizontal Axis Wind Turbines". PhD Thesis, Department of Mechanical Engineering, Monash University, (2005).

[13] Hillier, R. and Cherry, N.J., "The effects of stream turbulence on separation bubbles." Journal of Wind Engineering and Industrial Aerodynamics. (1981) Vol. 8: 49—58

[14] Li, Q.S. and Melbourne, W.H., "The effect of large-scale turbulence on pressure fluctuations in separated and reattaching flows." Journal of Wind Engineering and Industrial Aerodynamics. (1999) Vol. 83: 159-169

[15] Saathoff, P.J., "Effects of free-stream turbulence on surface pressure fluctuations in separated and reattaching flow". Ph.D. Thesis, Monash University, (1988).

[16] Melbourne, W.H., "Turbulence and the Leading Edge Phenomenon." Journal of Wind Engineering and Industrial Aerodynamics. (1993) Vol. 49: 45-64

[17] Mueller, T.J., Pohlen, L.J., Conigliaro, P.E. & Jansen Jr. B.J., "The influence of free-stream disturbances on low Reynolds number airfoil experiments." Experiments in Fluids. (1983) Vol. 1:3-14

[18] Ravi, S., Petersen, P., Watkins, S., Marino, M. and Watmuff, J., 'The Aerodynamic Performance and Flow Structure over a Flat-Plate Airfoil in Smooth and Turbulent conditions at Low Reynolds Numbers', Journal of Flow Visualization and Image Processing, (2011), Vol. 18, no. 3: 253-274

[19] Ravi, S., Watkins, S., Watmuff, J., Massey, K., and Petersen, P., 'Influence of Turbulence on Airfoil Performance at Low Reynolds Number'. (2012) AIAA Journal, (Accepted, In Press)

[20] Turbulent Flow Instrumentation see: http://www.turbulentflow.com.au

[21] Bergh H., & Tigdeman H., "Theoretical and experimental results for the dynamic response of pressure measuring systems", Rep. NLR-TR F.238, Jan. 1965

[22] Ravi, S., "The influence of turbulence on a flat plate airfoil at Reynolds numbers relevant to MAVs", PhD Thesis, School of Aerospace, Mechanical and Manufacturing Engineering, RMIT University, (2011).

[23] Ravi, S., Watkins, S., Watmuff, J., Massey, K., and Petersen, P., 'The flow over a thin airfoil subjected to elevated levels of freestream turbulence'. (2012) Exp. in Fluids, (Under Review)

Copyright Statement